# Neuro: Head and Neck Oncology

# 12

Martin W. Huellner, Spyros S. Kollias, Gerhard F. Huber, and Marcelo A. Queiroz

## Contents



M.W. Huellner (✉)
Department of Nuclear Medicine, University Hospital Zurich, Zurich, Switzerland
e-mail: martin.huellner@usz.ch

S.S. Kollias
Department of Neuroradiology, University Hospital Zurich, Zurich, Switzerland

G.F. Huber
Department of Otorhinolaryngology, Head and Neck Surgery, University Hospital Zurich, Zürich, Switzerland

M.A. Queiroz
Department of Nuclear Medicine, University of Sao Paulo, Sao Paulo, Brazil


A. Iagaru et al. (eds.), *PET/MRI in Oncology*,
https://doi.org/10.1007/978-3-319-68517-5_12

## 12.1 Introduction

Soon after the clinical implementation of PET/MR in 2011 and after initial feasibility studies, first comparative studies reported a draw between PET/MR and PET/CT with regard to the staging of head and neck cancer patients [1–8]. In the long run, however, PET/MR is expected to outstrip PET/CT in this field. This chapter aims to highlight current clinical applications and future directions of PET/MR in head and neck oncology.

PET/MR combines the advantages of molecular tumor imaging and high soft tissue contrast in one single examination—in contrast to the traditional approach, which often required both PET/CT and contrast-enhanced MR for a thorough workup of head and neck cancer patients. A more widespread clinical use of PET/MR is currently limited by monetary issues. On the one hand, the price for a PET/MR scanner including its requirements on building infrastructure is at least threefold the price of a PET/CT scanner. On the other hand, several countries are still lacking reimbursement models for PET/MR.

Centers with access to a PET/MR scanner generally prefer PET/MR over PET/CT in the initial staging of head and neck cancer patients—with the exception of cancers arising in the hypopharynx and larynx, where motion plays a prominent role, mainly swallowing [5]. For the nodal staging, both modalities are generally considered equivalent, although certain functional MR techniques might tip the scales toward PET/MR. The lung is the place where the majority of distant metastases of head and neck cancer patients occurs and was considered a black box for MR imaging for a long time [9]. Recent advances in the development of MR pulse sequences, some of them stimulated by the advent of PET/MR and its intrinsic need for proper lung tissue visualization, help elucidate this black box [10–13].

The scintigraphic imaging of malignant head and neck tumors today is mainly reserved to $^{18}$F-fluoro-2-deoxy-*D*-glucose (FDG). Other radiotracers might play a future role in the imaging of FDG-negative salivary gland malignancies, e.g., $^{68}$Ga-prostate-specific membrane antigen (PSMA); in neuroendocrine tumors, e.g., $^{68}$Ga-1,4,7,10-tetraazacyclododecane-1,4,7,10-tetraacetic acid (Tyr$^3$)-octreotate (DOTATATE); and in certain non-malignant neoplasms, e.g., $^{18}$F-fluorocholine (FCH) in parathyroid adenomas.

Proper photon attenuation correction (AC) is important in the head and neck, owing to oftentimes small-sized lesions of interest, narrow anatomical relationships, and a multitude a neighboring spaces and compartments. This is challenged by an abundance of tissues with different attenuation properties within a small and complex area and by the typical presence of artifacts elicited by dental hardware. Time-of-flight (TOF) PET dataset reconstructions are considered important in the head and neck, both for the detection and correct localization of small lesion but also for decreasing implant-related artifacts and for optimizing the MR-based AC [14–19]. While atlas methods can be used for the head in PET/MR, MR-based AC in the neck mainly relies on the Dixon method, which yields four different tissue properties (air, fat, water, soft tissue), but neglects the bone, which represents another black box for MR. In fact, bone assumes μ

map values similar to air, while the photon attenuation in both structures is entirely different. This issue might be overcome using MR pulse sequences with ultrashort echo time (UTE) or even—by definition—zero echo time (ZTE) [20–22].

## 12.2 PET/MR Protocols for the Head and Neck

The definition of valid protocols for PET/MR is a key requisite for clinical head and neck cancer assessment. MR pulse sequences should be selected to provide most complementary information or at least confirmatory information with regard to PET data. In integrated PET/MR scanners, the use of TOF PET information helps to identify small lesions, reduces artifacts—particularly those related to metallic implants such as dental hardware—and increases the accuracy of the MR-based AC [14, 15, 17–19]. For whole-body exams, the PET/MR protocol is divided into two separate, yet not independent, parts [23, 24]:

1. A fast basic whole-body oncologic PET/MR acquisition which contains the pulse sequence(s) used for MR-based AC, sufficient anatomic correlation, and basic soft-tissue characterization outside the head and neck area
2. A dedicated head and neck PET/MR acquisition that comprises high-resolution anatomical tumor imaging and enables the definition of specific tumor features, such as cellularity and vascularization

### 12.2.1 Basic Whole-Body PET/MR Acquisition

For the basic whole-body PET/MR acquisition, the patient should be positioned with arms down. The *Z*-axis scanning range covers the area from the vertex of the skull to the mid-thighs. A dedicated phased-array head and neck coil is used in conjunction with a body surface coil. PET datasets usually require 4–8 bed positions per patient (depending on the individual body height and on scanner geometry) of 2–5 min each (depending on scanner type and injected activity), using 3D image acquisition and reconstruction. The MR pulse sequences used for the AC are acquired during the PET acquisition. For the trunk, usually a T1-weighted Dixon-type sequence is used, whereas for the head, atlas methods may be used alternatively. Since the extremities are subject to wrapping artifacts in MR, AC of the extremities relies on PET data only. The same Dixon-type MR pulse sequence used for AC may also be used for diagnostic imaging, albeit with higher resolution. Repeating this pulse sequence after the administration of intravenous contrast is not essentially needed in head and neck cancer patients. If done, the acquisition takes place after the accomplishment of the non-contrast-enhanced MR pulse sequences of the head and neck. Using the phase-encoding gradient in anteroposterior direction helps reduce flow artifacts, especially in the posterior pharynx and larynx, although this requires a somewhat longer acquisition time [25].

Another diagnostic whole-body MR pulse sequence acquired is usually a T2-weighted image dataset, preferentially in coronal plane and with fat suppression, e.g., single-shot fast spin echo (SSFSE). One specific MR pulse sequence of the lung should also be part of this first step, especially in patients with a high likelihood of pulmonary metastases (higher T stage, lymph node metastasis in the lower neck, non-epithelial primary carcinoma, more than one primary tumor, etc.) [24, 26]. Most centers use a T2-weighted pulse sequence with motion correction, such as periodically rotated overlapping parallel lines with enhanced reconstruction (PROPELLER; GE Healthcare, Waukesha, WI). This sequence is acquired axially during free breathing and uses respiratory triggering [27, 28]. As an alternative, MR pulse sequences with ultrashort echo time or zero echo time may be considered. A recent study has shown that a free-breathing UTE pulse sequence has a high sensitivity for the detection of small pulmonary nodules (4–8 mm), including those not FDG-avid [29].

The PET acquisition and reconstruction covering the chest may take into account the respiratory motion in order to achieve an optimal standardized uptake value (SUV), particularly in small lung nodules and in lesions located in the base of the lungs. This can be accomplished using bellows-driven gating, MR-driven gating, or PET-driven gating [30]. This first part of the protocol can take from 12 to 25 min, depending on the parameters chosen for PET acquisition and MR pulse sequences.

### 12.2.2 Regional Head and Neck PET/MR Acquisition

A dedicated head and neck PET/MR protocol should not simply duplicate the clinical head and neck MR protocol routinely performed in the radiology department. A careful selection of MR pulse sequences is needed in order to optimize the diagnostic capability of PET/MR. The field of view and slicing of all regional MR pulse sequences need to be tailored to the head and neck and should not copy the parameters of the whole-body MR pulse sequences. Several studies have addressed the contribution of different MR pulse sequences for the assessment of head and neck tumors with PET/MR.

One typical recommendation is to acquire a T2-weighted sequence in at least two planes, using fat suppression, which gives sufficient information for tumor delineation. This can be supplanted with a T1-weighted sequence without fat suppression in at least one plane, preferably axial. This basic approach is already sufficient in many instances and avoids the injection of MR contrast medium [5]. However, this simple solution is not acceptable for presurgical planning, in stage T4 tumors, in recurrent tumors, and in cases of perineural spread [1, 5]. Here, contrast-enhanced fat-suppressed MR pulse sequences, acquired in at least two planes, are needed [1, 5, 24]. Since such a regional MR acquisition takes comparably long, a separate regional PET acquisition of the head and neck may be part of the protocol—making use of a long local bed time but without increasing the total examination time.

Functional MR sequences are also viable options for tumor characterization. This includes diffusion-weighted imaging (DWI), a surrogate marker of tumor cellularity, and perfusion-weighted imaging, a biomarker of vascularization and neoangiogenesis. Of note, information on tumoral glucose metabolism is already

available from FDG-PET and might obviate the need of such rather time-consuming functional MR pulse sequences. PET data may, e.g., be sufficient for therapy response assessment or the characterization of subcentimeter lymph nodes. Occasionally, FDG-avid pathologic lesions remain occult in areas with high physiologic glucose uptake, such as the lymphoepithelial tissue commonly found in the palatine tonsils and lingual tonsils. Here, functional MR pulse sequences, particularly DWI, assume a more prominent role. Recent studies analyzed the association of glucose metabolism, cellularity, and histological parameters in patients with squamous cell carcinoma and showed that DWI and FDG-PET may work as independent and complementary biomarkers [31–35]. Preliminary data are also available for perfusion-weighted imaging as part of a multiparametric PET/MR protocol for head and neck cancer. Covello and coworkers have proven the feasibility of such a protocol, which enables the simultaneous collection of metabolic and functional data [36]. Such a multiparametric approach may allow for a noninvasive characterization of tumor or recurrent tumor and might facilitate treatment planning.

Acquisition time, patient throughput, and individual patient tolerance are important issues to be considered. An advanced MR head and neck protocol takes about 30–35 min. Patients are instructed to breathe softly and not to swallow during the examination. Such is usually well tolerated. Notably, a multiparametric PET/MR acquisition may take longer, and the surface coils covering the head and neck as well as the torso might be uncomfortable and might preclude long acquisition times.

In summary, a regional PET/MR protocol for head and neck cancer should be tailored according to the specific questions that need to be answered. In most cases, the use of MR contrast medium is required, and functional MR sequences may not be needed. Specific parameters of MR pulse sequences have been suggested previously [24].

## 12.3 PET/MR Imaging of Carcinoma and Lymphoma in the Head and Neck

### 12.3.1 T Staging

More than 90% of all head and neck carcinomas are of squamous cell histology. The risk factors for this type of tumor comprise smoking and alcohol in general (exponential risk), and certain viral oncogenes in specific subsets, such as Epstein-Barr virus (EBV) in the nasopharynx and human papillomavirus (HPV) in younger patients, mainly in the oropharynx.

When a patient is referred for the initial imaging staging of a head and neck tumor, typically the tumor has already been identified, and good estimates have been made on its local extension and potential infiltration of adjacent structures [37, 38]. There is ample literature on comparing PET/CT and MRI for the local staging of tumors, which basically shows that MRI identifies the tumor extent more accurately, owing to better soft tissue contrast [37]. On the other hand, MR has also been compared with PET/MR, and most authors found no significant difference in the assessment of primary tumors [5, 39]. Based on these findings, one would expect a higher accuracy of

PET/MR than PET/CT in the T staging of head and neck carcinomas, but this is controversial. Most studies performed with sequential or simultaneous PET/MR scanners could not prove superiority of PET/MR over PET/CT [1, 3, 5, 6, 8]. Vice versa, this means that PET could compensate for the known shortcomings of CT in the head and neck [1]. If MR contrast medium cannot be injected, PET/MR using only T2-weighted neck imaging yields similar accuracy as contrast-enhanced PET/CT [5].

In our opinion, the imaging of head and neck tumors requires a more specific approach. Data derived from studies, where tumors from several sites in the head and neck are literally lumped together, need to be regarded with caution. A site-specific comparison of modalities is desired, but data in the literature is currently sparse. Site-dependent differences in the accuracy of PET/CT and PET/MR are expected to arise from the anatomical component, i.e., CT or MR, respectively, since uptake measurements are comparable and reproducible among both modalities [4, 40].

It is expected that tumors arising in the oral cavity and in the oropharynx should better be imaged with PET/MR than with PET/CT, owing to less artifacts from dental hardware on MR than on CT and higher soft tissue contrast of MR (Fig. 12.1) [5, 41]. The PET data is compromised both by dental artifacts on CT and MR, which deteriorate the AC—although on PET/MR purportedly to a lesser extent than on PET/CT [17, 19, 42, 43]. The puffed cheek approach has not been studied on PET/MR so far and is expected to be more challenging owing to longer regional acquisition time with PET/MR [44]. Tumors hiding within tissue with physiologically high FDG uptake, such as lymphoepithelial tissue, which might be abundant in the oropharynx, can be missed with PET/MR, unless DWI is used [8, 45–48].

In the hypopharynx and larynx, the situation is expected to be different. Artifacts there mainly derive from patient motion, such as swallowing or breathing [5, 49]. The soft tissue contrast of CT in this area is sufficient, owing to comparably sharp density increments between the tissues there, such as intralaryngeal air, laryngeal muscles, paraglottic fat, laryngeal cartilage/ossified cartilage, and paralaryngeal fat and muscles.

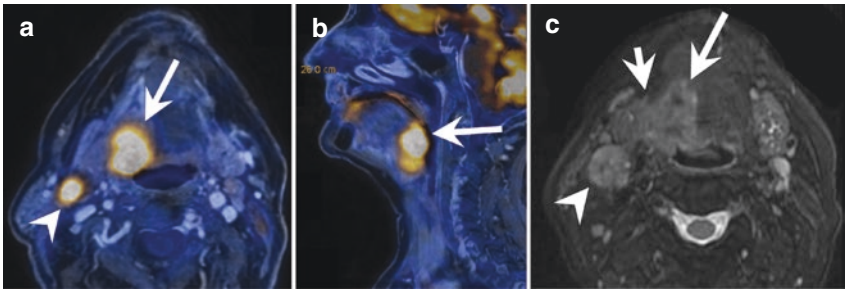


**Fig. 12.1** Squamous cell carcinoma arising in the oropharynx. The axial contrast-enhanced, fat-suppressed T1-weighted $^{18}$F-FDG-PET/MR image shows an intensively FDG-avid tumor in the base of the tongue on the right side (**a**, *arrow*) and an FDG-avid lymph node metastasis in cervical level IIA (*arrow head*). The tumor extends from the tongue base to the vallecula, as seen on the sagittal T1-weighted $^{18}$F-FDG-PET/MR image (**b**, *arrow*). On the fat-suppressed T2-weighted image, the tumor is of inhomogeneous signal intensity with predominant hyperintense areas compared to muscle (**c**, *long arrow*) and infiltrates the intrinsic and extrinsic tongue musculature (**c**, *long arrow*) as well as the parapharyngeal adipose tissue and the right-sided submandibular gland (**c**, *short arrow*). The lymph node metastasis is seen as well (**c**, *arrow head*)

Additionally, CT offers higher spatial resolution. Thus, PET/CT might remain the modality of choice for the imaging of hypopharyngeal and laryngeal tumors, especially for smaller ones—although hybrid imaging is performed uncommonly in T1 tumors, and such small tumors might be missed completely with any imaging modality [5, 50]. There are, however, also studies with small patient cohorts that showed a similar performance of PET/MR and PET/CT in the staging of laryngeal carcinoma [51].

The potential resectability of head and neck tumors depends on several issues [52]. Not all of them are part of the TNM staging system, and if they are part, they not necessarily denote a T4b stage, which is generally considered unresectable. Particularly, the following findings with a head and neck tumor might preclude surgery or lead to a different surgical approach: vascular encasement, invasion of the prevertebral space, perineural spread, orbital invasion, bone infiltration, skull base invasion, dural infiltration, invasion of the laryngeal cartilage, invasion of the brachial plexus, and mediastinal invasion (Fig. 12.2). For all of these items, except bone and cartilage infiltration, PET/MR is expected to yield a higher accuracy than PET/CT, although evidence is currently sparse [1, 5, 53]. Particularly in cases of perineural spread, PET/MR is expected to be more accurate, owing to the higher soft tissue contrast of MR and the availability of differently weighted images [5, 37, 53]. Both contrast-enhanced MR pulse sequences with and without fat suppression may be used for this purpose in general, but preferably non-suppressed sequences should be used in the skull base [38, 54].

PET/MR provides no advantage over PET/CT in specifying FDG-positive incidental findings in the head and neck area [55]. Wang and colleagues showed that FDG-PET/MR can be used for radiation therapy planning in the head and neck, yielding similar gross tumor volumes as contrast-enhanced CT [56].

It is generally agreed upon that local tumor recurrence is best assessed with PET/MR [39, 57–59]. PET/CT is limited in identifying a morphological correlate for focal FDG uptake in the postsurgical head and neck [57, 58]. While PET may guide biopsy in such cases, biopsy might be difficult in lesions that are located in so-called blind spots, e.g., the piriform sinus or the postcricoid area, or if submucosal tumor recurrence is suggested and in-depth biopsy (e.g., using laser) is required. On the other hand, muscle tissue of surgical flaps or orthotopic muscle adjacent to such flaps might present with unusual and remarkable FDG uptake, owing to increased muscle tone as a consequence of the altered anatomy in the postsurgical state [37, 60, 61]. The higher soft tissue contrast of MR allows for a more specific assessment of focal FDG uptake identified on follow-up exams of head and neck cancer patients and for a more reliable discrimination of normal muscle and recurrent tumor [24, 37, 39, 48, 57, 59]. Additionally, DWI may be helpful, particularly in irradiated patients [24, 47, 48, 62].

### 12.3.2 N Staging

The presence of nodal metastases is a very important and independent prognostic factor, which worsens the prognosis of head and neck cancer patients [37]. One single lymph node metastasis already decreases the overall survival by approximately 50% [37, 63–65]. The prognosis worsens with the number of lymph nodes

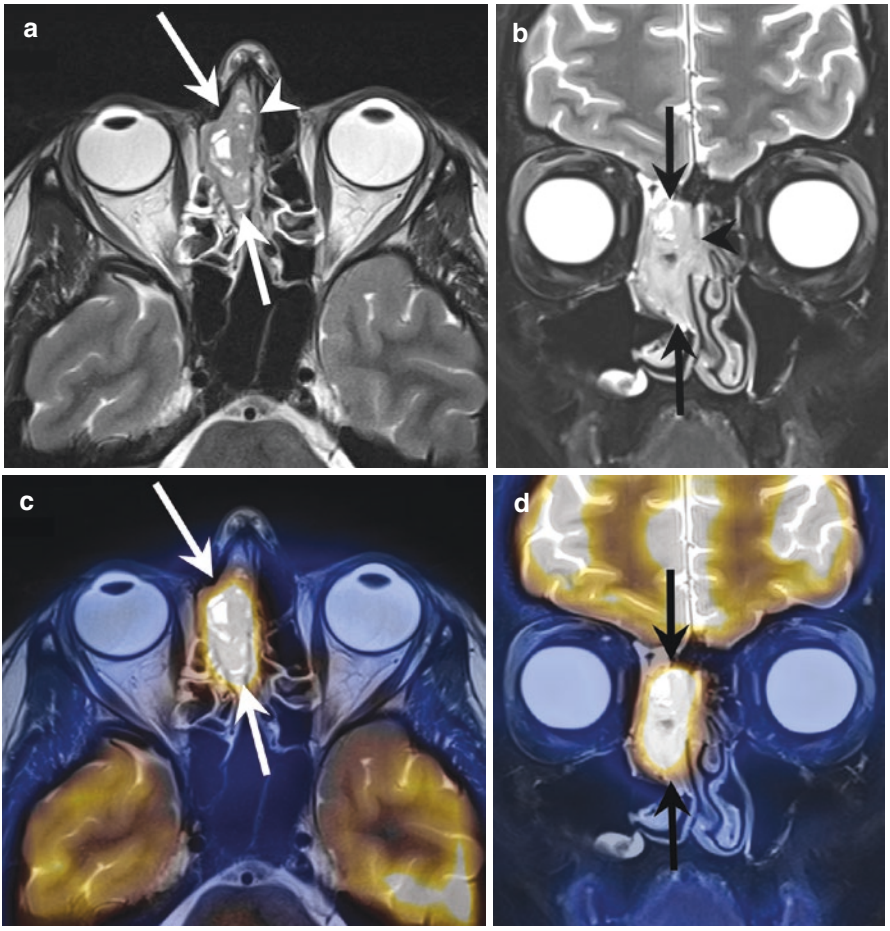


**Fig. 12.2** Esthesioneuroblastoma arising in the ethmoid air cells. The axial non-suppressed (**a**) and coronal fat-suppressed (**b**) T2-weighted images show a tumor (*arrows*) in the right-sided ethmoid air cells. The tumor is of intermediate signal intensity and contains cystic spaces. The osseous nasal septum is infiltrated (*arrow head*). No extension into the orbita or infiltration of the dura is seen; the nasal bone is preserved. The axial non-suppressed (**c**) and coronal fat-suppressed (**d**) T2-weighted $^{18}$F-FDG-PET/MR images confirm high FDG uptake of the tumor (*arrows*) and absence of pathologic FDG uptake in the orbit

involved, with presence of extracapsular spread, and with pathologic nodes in the lower neck (e.g., level IV) [37, 64–67].

The probably most important tool in the N staging with hybrid imaging is PET, no matter if combined with CT or with MR. Therefore, most studies could not provide evidence that PET/MR surpasses PET/CT in this field [1, 4, 6, 53, 68, 69]. This reflects various previous works on PET/CT, MR, and CT, where a similar accuracy of modalities was found, ranging from approximately 60% to 90% with regard to sensitivity and specificity [9, 37, 50, 70–72]. One possible advantage of PET/MR could lie in the more accurate staging of small nodes, especially those with necrotic

or cystic centers (e.g., with human papillomavirus subtypes 16, 18, or 31), since these might be faintly FDG-avid or even not avid but are more easily identified on fat-suppressed T2-weighted MR images than on CT [37, 73–75]. Another advantage of PET/MR might be the possibility to acquire a regional PET dataset with higher resolution during the regional MR exam, without increasing the total acquisition time. This might help identify small pathologic nodes. The use of DWI does not increase the accuracy of nodal staging with PET/MR [62].

### 12.3.3 M Staging and Second Primaries

Approximately 10% of all head and neck cancer patients have distant metastases upon initial presentation [37]. Per year, another 5% of patients develop second primary tumors due to field cancerization. The most common site of distant metastases and second primaries in patients with head and neck cancer is the lung [9]. Therefore, PET/MR in head and neck patients should also incorporate adequate lung imaging (see above). Studies have shown that MR lung sequences used in PET/MR, e.g., PROPELLER, detect lung nodules of 3 mm [10, 29]. Moreover, more than 98% of all FDG-negative subcentimeter lung nodules are benign, and 97% of lung nodules missed on PET/MR do not grow [76, 77]. For a more detailed discussion of lung nodules, we refer to Chap. 15 of this book.

Another common site for metastases is the skeleton. Here, some studies with general oncological cohorts reported a higher confidence in PET/MR than PET/CT, although no significant difference was found [2, 78, 79]. Specific studies on bone metastases in head and neck cancer patients today are missing.

Altogether, the majority of the currently published studies report a similar accuracy of PET/CT and PET/MR in the M staging of head and neck cancer patients [1, 2, 4, 36]. An overview on published major PET/MR studies is given in Table 12.1.

### 12.3.4 Lymphoma

The most common type of primary lymphoma of the head and neck region is non-Hodgkin lymphoma (NHL). Approximately 90% of NHL of the head and neck are of B-cell lineage, while only 10% are of T-cell lineage [80]. Tumors are mainly located in the oral cavity, in the nasal cavity, in the paranasal sinuses, and in major salivary glands (Fig. 12.3). Approximately one third of head and neck lymphomas arise in the bone, one third in soft tissues, and one third in multiple structures [80]. More than half of head and neck lymphomas come without pathologic lymph nodes, while in the rest nodal involvement may skip anatomical levels. Sinonasal lymphoma most often manifests as diffuse large-cell B-cell lymphoma (DLBCL), followed by NK/T-cell lymphoma. Sinonasal lymphoma typically presents as a comparably homogeneous mass that is of intermediate signal intensity on T1-weighted images and of high signal intensity on T2-weighted images. Hodgkin lymphoma often also involves neck lymph nodes, but disease is typically not limited to the neck, but occurs also in the mediastinum and sometimes in the spleen.

**Table 12.1** Overview on published major prospective studies in PET/MR of the head and neck, as of May 2017

| First author | Year published | PET/MR scanner type | Number of subjects in study | Main findings | Reference number |
|---|---|---|---|---|---|
| Schaarschmidt | 2017 | Simultaneous | 81 | Incidental tracer uptake in the head and neck cannot be classified more accurately with PET/MR than with PET/CT | [55] |
| Wang | 2017 | Simultaneous | 11 | Gross tumor volume derived by PET/MR and CT is similar in oropharynx carcinoma patients, reverting into similar radiation doses | [56] |
| Sekine | 2017 | Sequential | 58 | PET/MR and PET/CT are reliable in defining head and neck tumor resectability | [53] |
| Cavaliere | 2017 | Simultaneous | 16 | PET/MR is useful for the initial staging of laryngeal cancer | [51] |
| Sekine | 2017 | Sequential | 27 | Whole-body staging with PET/MR yields at least equal diagnostic accuracy as PET/CT in head and neck cancer patients | [1] |
| Rasmussen | 2017 | Simultaneous | 21 | DWI and FDG-PET from PET/MR yield similar radiation therapy volumes. FDG uptake and DWI do not correlate | [32] |
| Schaarschmidt | 2016 | Simultaneous | 25 | PET/MR and PET/CT perform equally well in tumor staging and tumor recurrence assessment | [3] |
| Surov | 2016 | Simultaneous | 11 | ADC and SUV are correlated with different histopathological parameters, enabling their use as complementary biomarkers in head and neck squamous cell carcinoma | [31] |

**Table 12.1** (continued)

| First author | Year published | PET/MR scanner type | Number of subjects in study | Main findings | Reference number |
|---|---|---|---|---|---|
| Covello | 2015 | Simultaneous | 44 | PET/MR is feasible for tumor staging and tumor recurrence assessment | [36] |
| Rasmussen | 2015 | Simultaneous | 30 | FDG uptake in PET/CT and PET/MR is identical and highly reproducible | [40] |
| Varoquaux | 2014 | Sequential | 32 | PET/MR and PET/CT are equal in terms of image quality, lesion conspicuity, and lesion localization in head and neck cancer patients | [8] |
| Platzek | 2014 | Sequential | 38 | PET/MR is equal to PET and MR in nodal staging | [69] |
| Queiroz | 2014 | Sequential | 87 | PET/MR is preferred over PET/CT in the workup of head and neck tumor recurrence | [57] |
| Partovi | 2014 | Sequential | 14 | PET/MR and PET/CT are equal in nodal staging and detection of distant metastases in head and neck cancer patients | [4] |
| Kuhn | 2014 | Sequential | 150 | T2-weighted PET/MR is at least equal to contrast-enhanced PET/CT | [5] |
| | | | | Contrast-enhanced T1-weighted PET/MR is superior to T2-weighted PET/MR with regard to tumor delineation, infiltration of adjacent structures, and perineural spread | |
| Kubiessa | 2014 | Simultaneous | 17 | PET/MR and PET/CT perform identically | [6] |
| Queiroz | 2014 | Sequential | 188 | DWI as part of PET/MR does not provide important additional information for tumor staging | [62] |
| Platzek | 2013 | Sequential | 20 | PET/MR is feasible for head and neck tumor imaging | [7] |

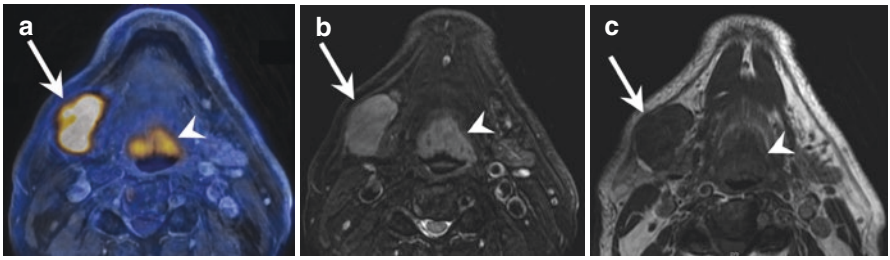


**Fig. 12.3** Primary lymphoma of the head and neck, arising from the inferior portion of the submandibular gland. An intensively FDG-avid lesion is seen in the angle of the mandible on the right side on contrast-enhanced, fat-suppressed T1-weighted $^{18}$F-FDG-PET/MR image (**a**, *arrow*). The lesion is homogeneously hyperintense on the fat-suppressed T2-weighted image (**b**, *arrow*) and isointense to muscle on the T1-weighted image (**c**, *arrow*). No perilesional stranding is seen in the subcutaneous or parapharyngeal adipose tissue. The lesion displaces the superior portion of the right-sided submandibular gland. Normal lymphoepithelial tissue with moderate FDG uptake is seen as well (*arrow heads* on **a**–**c**)

Specific PET/MR studies on head and neck lymphoma are currently lacking. PET/MR experience in more general lymphoma cohorts shows that SUVs from PET/CT and PET/MR are strongly correlated [81]. Apparent diffusion coefficient (ADC) values of lymphoma are unrelated to the SUV, which supports the assumption that both parameter sets represent independent biological information [81]. The diagnostic capability of PET/CT and PET/MR is similar and exceeds whole-body MR imaging with DWI [82]. For a more extensive discussion of PET/MR imaging of lymphoma, we refer to Chap. 22 of this book.

In summary, PET/MR has advantages over PET/CT in tumors arising in the oral cavity and in the oropharynx, as well as in recurrent tumors. The one-stop-shop opportunity, the future optimization of MR-based attenuation correction, the incremental use of MR artifact reduction techniques, and the advancement of MR pulse sequences dedicated to lung imaging might emphasize the role of PET/MR in the imaging of head and neck carcinoma and lymphoma.

## 12.4 PET/MR Imaging of Thyroid Carcinoma and Other Head and Neck Malignancies

The therapy of differentiated thyroid carcinoma requires thyroidectomy along with postoperative radioiodine therapy in most cases. Once there is a suspicion of recurrence, e.g., with rising levels of thyroglobulin, the detection and localization of recurrent tumor is mandatory in order to guide treatment. Recurrence may occur in the thyroid bed, in regional lymph nodes and soft tissues, or uncommonly in distant sites. The search for recurrent tumor is usually performed with hybrid imaging modalities, such as $^{123}$I-SPECT/CT or $^{18}$F-FDG-PET/CT in case of suspected dedifferentiation. However, abnormal focal radioiodine uptake or $^{18}$F-FDG uptake may be present without an obvious pathomorphological correlate in thyroid carcinoma

patients. This can be either because the pathologic lesions are below the spatial resolution of CT or because of certain limitations of the CT protocol. The CT is usually acquired as "low-dose" scan, and ideally without intravenous iodinated contrast, which would render a subsequent radioiodine therapy futile for a couple of weeks.

In this regard, $^{124}$I-PET/MR gained some ground. This modality allows for a better morphological correlation than PET/CT for characterizing neck tissue, especially in lesions smaller than 10 mm, thereby improving the pretherapeutic lesion dosimetry [83]. These results are not completely reflected in more recent work, where $^{124}$I-PET/MR was indeed superior to PET/CT in detecting iodine-positive lesions, although this remains arguable [84, 85]. Yet, $^{124}$I-PET/MR could not distinguish thyroid remnant from metastasis, while the volumetric MR information was considered useful for dosimetry purposes [84, 85].

In another study, $^{18}$F-FDG-PET/MR yielded an accuracy similar to contrast-enhanced $^{18}$F-FDG-PET/CT in patients with suspicion of dedifferentiated thyroid cancer, except for the detection of lung nodules, where PET/CT was superior [86]. Thus, PET/MR using either $^{124}$I or $^{18}$F-FDG is recommended at the moment only in cases of pretherapeutic dosimetry and when the use of iodine-based contrast medium is contraindicated. In all other clinical scenarios, PET/CT should be preferred, which also provides shorter acquisition time, better cost-effectiveness, and a somewhat more accurate AC [87].

On the other hand, parathyroid hyperplasia of single or multiple glands might be well addressed with PET/MR using $^{18}$F-fluorocholine (FCH), which might be useful both for diagnosis and pretherapeutic planning (Fig. 12.4) [88]. A prospective pilot study investigated the performance of $^{18}$F-FCH-PET/MR imaging in ten patients with biochemical primary hyperparathyroidism and inconclusive results at ultrasound and $^{99m}$Tc sestamibi scintigraphy. This small study reported a sensitivity of 90% for PET/MR in this challenging patient cohort, without any false-positive results, allowing for an accurate localization of adenomas and providing detailed anatomic information [89].

Other rare tumors of the head and neck, such as those with neuroendocrine differentiation (paragangliomas) and meningiomas, may also be imaged with PET/MR, especially in conjunction with somatostatin analogue radiotracers, such as $^{68}$Ga-1,4,7,10-tetraazacyclododecane-1,4,7,10-tetraacetic acid (Tyr$^3$)-octreotate (DOTATATE). The combination of specific morphological features of these tumors together with $^{68}$Ga-DOTATATE uptake allows for an accurate diagnosis and also opens the opportunity for peptide receptor radionuclide therapy, e.g., with $^{177}$Lu-DOTATATE, if surgery is not possible [24, 90].

More recently established clinical imaging using $^{68}$Ga-labeled prostate-specific membrane antigen (PSMA) might gain importance in salivary gland malignancies, owing to the comparably high physiologic uptake of $^{68}$Ga-PSMA in salivary gland tissue. While the primary tumor within the gland and its extent is delineated by the MR component of PET/MR, pathologic lymph nodes and distant metastases are possibly identified using $^{68}$Ga-PSMA-PET [91]. This novel radiotracer might play a role especially in those neoplasms, which generally show only faint $^{18}$F-FDG uptake, such as adenoid cystic carcinoma or acinic cell carcinoma [24, 49]. However, comparative studies are currently lacking.

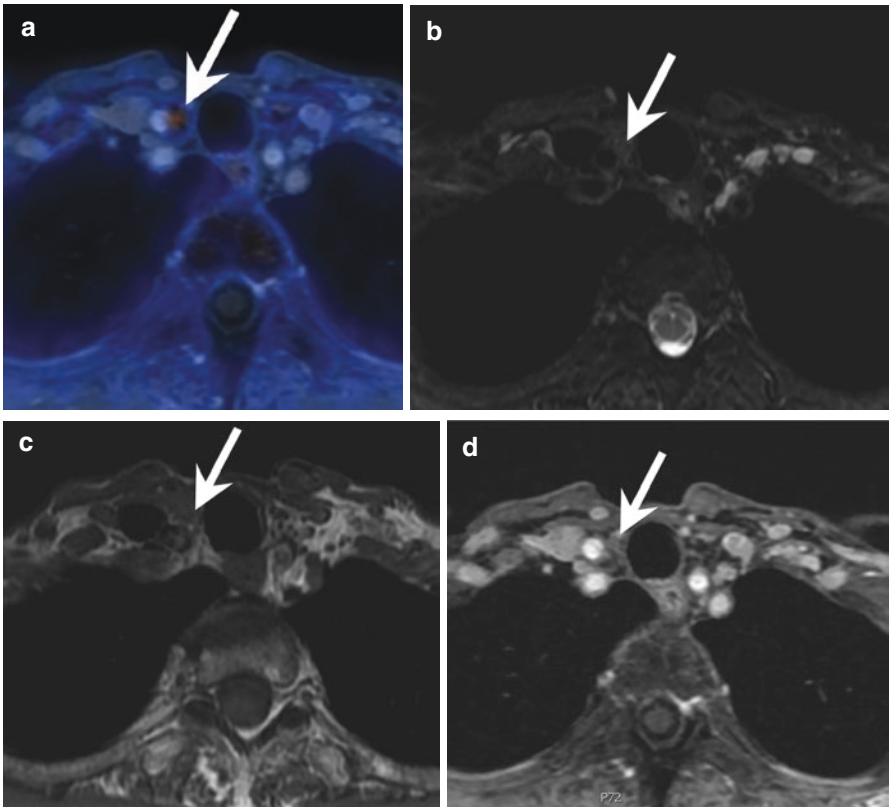


**Fig. 12.4** Parathyroid adenoma in a patient with hyperparathyroidism and negative ultrasound and negative dual-isotope subtraction SPECT/CT. A tiny choline-positive nodule is seen below the right thyroid lobe on contrast-enhanced, fat-suppressed T1-weighted $^{18}$F-FCH-PET/MR image (**a**, *arrow*). The nodule is isointense to muscle on the fat-suppressed T2-weighted image (**b**, *arrow*), hardly visible as isointense to muscle on the T1-weighted image (**c**, *arrow*), and does not take significant contrast on the contrast-enhanced, fat-suppressed T1-weighted image (**d**, *arrow*)

In summary, the use of PET/MR in head and neck oncology might exceed the traditional assessment of head and neck squamous cell carcinoma with $^{18}$F-FDG. The advent of different tracers in the last decade together with the diagnostic capability of MR in lesion detection and characterization may facilitate the dissemination of PET/MR for the imaging of various types of tumors that occur in the head and neck.

## 12.5 Multiparametric PET/MR

PET/MR in head and neck cancer is mainly performed for one or more of the following reasons: TNM staging, surgery or radiotherapy planning, prognostic information, therapy response assessment, and detection of tumor recurrence. As with

anatomical MR pulse sequences, the use of functional MR pulse sequences should depend on the pertinent clinical information and questions to be answered, in order to optimize the study time and prevent a redundancy of information. The following paragraphs discuss the most commonly used functional MR pulse sequences that might enhance the diagnostic accuracy of PET/MR in head and neck cancer (Fig. 12.5). A summary of the potential benefits of each discussed MR pulse sequence in comparison to the obligatory PET is given in Table 12.2.

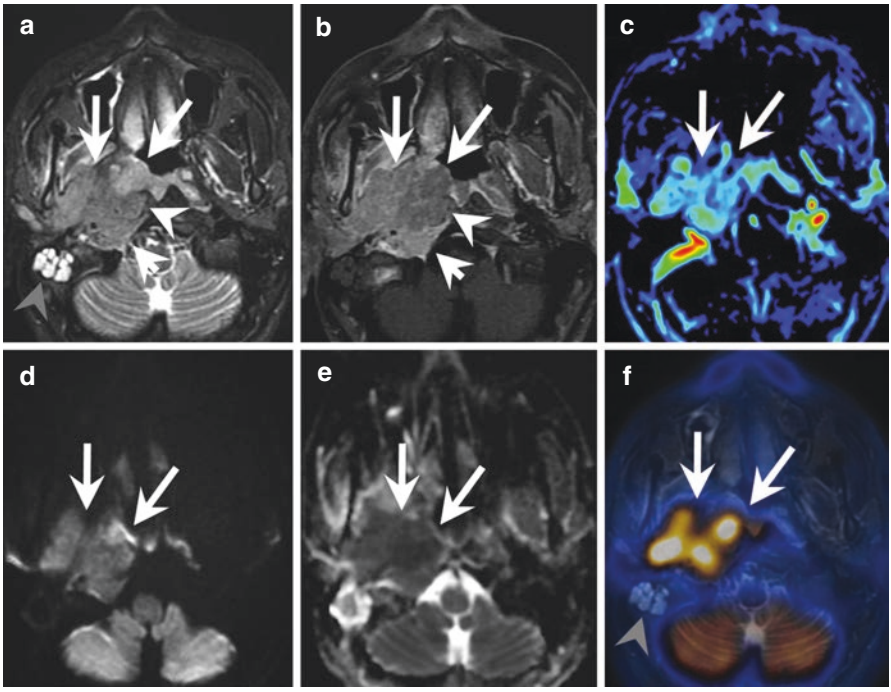


**Fig. 12.5** Squamous cell carcinoma of the nasopharynx. Multiparametric PET/MR acquisition including axial T2-weighted image (**a**), contrast-enhanced T1-weighted image with fat suppression (**b**), perfusion-weighted image map of maximum slope of increase (**c**), diffusion-weighted image (**d**) and corresponding ADC map (**e**), as well as co-registered T2-weighted $^{18}$F-FDG-PET/MR image (**f**) shows a heterogeneous FDG-avid tumor in the right-sided lateral wall of the nasopharynx (*arrows* on **a–f**). The tumor infiltrates the prevertebral muscles (*arrow head* on **a**, **b**), the right-sided hypoglossal canal (*short arrow* on **a** and **b**), the clivus, the parapharyngeal space including the carotid space, and the masticator space. FDG-negative fluid retention in the right-sided mastoid air cells (*gray arrow* on **a**, **f**) indicates obstruction of the Eustachian tube by the tumor and should not be confused with mastoiditis. Vascularization of the tumor is rather poor (**c**), indicating unfavorable response to treatment. The tumor shows restricted diffusion (**d**, **e**), compatible with high cellularity, and corresponding to poor differentiation, as revealed by subsequent histopathology. Several enlarged and FDG-avid lymph nodes were also seen on the right side (not shown)

**Table 12.2** MR pulse sequence benefits in different clinical scenarios in comparison with PET imaging

| Imaging component | Clinical task | | | | | |
|---|---|---|---|---|---|---|
| | Tumor detection | Surgery planning | Radiotherapy planning | Prognostication | Therapy response assessment | Detection of tumor recurrence |
| FDG-PET | ++ | ++ | ++ | + | ++ | ++ |
| DWI | + | – | + | ++ | + | + |
| DCE | – | – | – | ++ | + | + |
| Spectroscopy | – | – | – | + | (+) | (+) |
| BOLD | – | – | – | + | – | – |
| SPIO | + | + | – | – | – | – |

– means no value; (+) means potential indication; + means limited use; ++ means clinically useful

### 12.5.1 Diffusion-Weighted Imaging (DWI)

Application of DWI in MR exams for head and neck cancer has been extensively studied and is used for several indications that can be roughly divided into two different scenarios: before and after treatment. The pretreatment scenario provides information on primary tumor location, on nodal status, for therapeutic planning, and for the prediction of treatment response. In the posttreatment scenario, DWI is used for the assessment of therapy response and discrimination of post-therapeutic changes and tumor recurrence.

A recent meta-analysis showed no added value of DWI in detecting the primary tumor but a potential role in nodal staging, allowing the differentiation of benign and metastatic cervical lymph nodes [92]. As to PET/MR, this information is already contained in the $^{18}$F-FDG-PET component yet with a higher level of purity [62]. Moving from macroscopic imaging tasks, such as staging, to microscopic imaging tasks, the situation is different. For the assessment of specific features of tumors and lymph nodes, such as their histopathological profile, it was shown that DWI provides information that is complementary to the PET-derived information, similarly as shown before in other parts of the body [31]. Some tumor characteristics, such as high stromal content and low cellularity, are associated with resistance to treatment and increased water diffusivity in head and neck cancers. Thus, in general, high mean ADC values are considered predictors of poor treatment response and outcome [93]. Studies investigating DWI parameters and clinical outcome have shown that high ADC values both in primary tumors and metastatic lymph nodes were able to predict tumor relapse, failure of regional control, and poor disease-free survival [94, 95]. On the other hand, poorly differentiated squamous cell carcinoma usually presents low ADC values and is at higher risk for metastatic disease, being another independent biomarker of poor treatment response [96]. This controversy confirms that prognostication by means of quantitative DWI parameters should be regarded with caution.

For therapeutic planning, DWI has been studied for dose painting in comparison to $^{18}$F-FDG-PET. It has been shown that both techniques contain different

information, which might influence the target volumes of radiotherapy [97]. Similarly, Rasmussen and colleagues have recently assessed the overlap of the radiation therapy volume of interest, as measured with DWI and $^{18}$F-FDG-PET by multiparametric PET/MR in patients with head and neck cancer [32]. They showed that the target volume for radiotherapy overlapped substantially, although not completely, suggesting that glucose uptake and diffusion coefficient yield complementary information, which may be relevant for radiotherapy treatment planning [32].

DWI after treatment provides valuable information for therapy response assessment. A rising ADC value, which may be more reproducible than a single measurement, was described as an early biomarker of response to treatment and might play a role when gadolinium cannot be used [98–100]. Treatment-related changes in the head and neck region after surgery and radiotherapy limit the discriminability between viable tumor and therapy-induced inflammation. In this regard, DWI might tip the scales by showing significant lower ADC values in tumors compared to posttreatment changes, especially when using high b-values (higher than 1000 s/mm$^2$) [101, 102].

Some technical issues of DWI need to be addressed. The lack of standardization, such as the choice of b-values and the method to draw the ROI, and the high prevalence of artifacts (susceptibility and movement) might hamper the image acquisition and quality, limiting its reproducibility interindividually and intraindividually [93].

In summary, DWI plays a more complementary than redundant role in the assessment of head and neck cancer using $^{18}$F-FDG-PET/MR, with potential clinical benefits in differentiating benign from malignant disease, particularly in the restaging after treatment (recurrence vs. inflammation). It may also play a role for therapy response assessment—provided the protocol is standardized and pertinent thresholds are being established and validated in future studies.

### 12.5.2 Perfusion-Weighted Imaging

Dynamic contrast-enhanced (DCE) sequences and dynamic susceptibility contrast (DSC) sequences are MR techniques targeting tissue perfusion. They are performed after the intravenous injection of contrast medium. Both techniques depict the vascular properties of a lesion, serving as an imaging biomarker of neoangiogenesis and hypoxia, which can be used to characterize a tissue as malignant and also to predict treatment failure. In head and neck oncology, lesions with high perfusion parameters generally tend to show better response to treatment, probably owing to more appropriate delivery of the therapeutic agents, but are more likely to develop hematogenic metastasis. Some parameters can be extracted from perfusion-weighted MRI, both quantitative parameters such as $k^{trans}$ (derived through pharmacokinetic models) and semiquantitative parameters (analyzed by the time-signal intensity curve). Several parameters were studied in different clinical settings.

Two main applications of perfusion-weighted MRI in head and neck oncology are identified: pretreatment prognostic information and, more commonly, therapy response assessment. In general, high $k^{trans}$ values both in primary tumors and in metastatic lymph nodes are related to favorable treatment response [103–105].

However, the lack of standardization of image acquisition and analysis renders perfusion-weighted MRI challenging, with oftentimes limited reproducible.

On the other hand, head and neck tumors with higher vascularization are candidates to assess treatment response with perfusion-weighted MRI. In these tumors, perfusion parameters might allow an accurate identification of patients with improved response to chemotherapy and radiotherapy and prolonged survival. This is a reflection of the association of high blood flow and increased oxygenation, resulting in better delivery of the antineoplastic agents and increased radiosensitivity [103]. Even more important, change in $k^{trans}$ after therapy is much more consistent than the pretreatment measurement. Recent studies provide preliminary data on the parametric response map as an early predictor of treatment efficacy in head and neck cancer and also highlight the potential of posttreatment DCE-MRI in identifying residual masses [106–108]. Thus, perfusion parameters could help to individualize therapy, avoiding unnecessary treatment and improving patient survival.

In conclusion, similarly to DWI, perfusion-weighted MR imaging has a potential role in the multiparametric analysis of head and neck cancer. Its preferred applications are most likely the prediction of response to treatment by identifying primary tumors with high blood flow and the anticipation of resistance to chemotherapy and radiation therapy.

### 12.5.3 Other Functional MR Techniques (MR Spectroscopy, IVIM, and BOLD)

A selection of other functional MR pulse sequences may also aid in the assessment of head and neck cancer. Care should be taken on which MR sequence is essential for the PET/MR examination and which could benefit patient management without increasing the scanning time. Otherwise, the translation of PET/MR into clinical routine would be impaired, and PET/MR might only be reserved for special (and rare) occasions.

One of the first functional sequences studied was MR spectroscopy (MRS). Although challenging due to long acquisition time and complex post-processing and analysis, MRS might play a role in tumor prognostication and in monitoring treatment response [109]. High choline-to-creatine ratios in primary head and neck tumors were observed in patients with poor response to therapy [110]. In the posttreatment scenario, the presence of a choline peak in a residual mass may serve as a marker of residual cancer [111]. However, there are only a few and small studies addressing the role of MRS in head and neck cancer. Therefore, one should take into account the imaging time available and the expected findings before considering including MRS into a PET/MR protocol.

The intra-voxel incoherent motion (IVIM) represents an MR technique that allows the simultaneous evaluation of vascularization and diffusion restriction without the use of contrast medium [112]. Thus, the potential applications of DWI and MR perfusion might be covered with a single acquisition. IVIM can be used to

characterize head and neck primary tumors and metastatic lymph nodes [113]. It was also shown useful for monitoring therapy response, where high perfusion parameters were associated with worse clinical outcome, and an increase in IVIM parameters (e.g., diffusion coefficient D) was observed in responders [114, 115]. However, in our experience IVIM still suffers from considerable field inhomogeneities in PET/MR imaging and complex post-processing in general.

Blood-oxygen-level-dependent (BOLD) MR imaging is an indirect biomarker of tumor hypoxia, which might reflect resistance to chemotherapy and radiotherapy of head and neck cancer and consequently poor outcome. The principle of BOLD imaging in oncology is based on tumor oxygenation. It measures the decrease of signal intensity on T2*-weighted images owing to the paramagnetic effect of deoxyhemoglobin [93]. Although promising, feasible, and potentially reproducible, research effort still is needed to prove its efficacy in a clinical environment.

Another potential utility of MR imaging is the use of superparamagnetic iron oxide (SPIO) as contrast agent. Although only preliminary data is available to date, SPIO MR was shown able to distinguish benign and malignant lymph nodes, which is oftentimes difficult with conventional cross-sectional imaging in lesions smaller than 1 cm [116]. Such might be useful if the information derived from $^{18}$F-FDG-PET is equivocal.

In summary, the aforementioned functional MR sequences have yet not translated into clinical routine at most centers. They are time-consuming and their reproducibility is often limited. IVIM has been extensively studied for therapy response assessment and may be considered clinically in the future, provided more stable acquisition and faster post-processing are available. BOLD imaging might be used to predict response to treatment but still lacks consistent literature. MRS is technically challenging and might be considered mainly for research purposes. Thus, the implementation of such MR pulse sequences as part of a clinical PET/MR protocol remains questionable, given the compulsory presence of $^{18}$F-FDG-PET. Another counterargument is the availability of different radiotracers that image similar biologic processes, such as $^{18}$F-fluoroazomycin arabinoside (FAZA) or $^{18}$F-fluoromisonidazole (FMISO) for hypoxia estimation [117–119].

## 12.6 Summary

The use of PET/MR gains ground on PET/CT for the assessment of head and neck tumor patients. Once certain technical challenges are solved, such as a further improvement of lung imaging and more robust attenuation correction methods, e.g., by using zero echo time MR pulse sequences, a stable and reliable clinical hybrid imaging modality is at hand. This happens parallel to the clinical implementation of new PET radiotracers, the validation of existing clinical PET radiotracers for new indications (e.g., parathyroid imaging with $^{18}$F-fluorocholine), and an increase in the availability of functional MR techniques. Altogether, there is prospect of a more sophisticated and complementary characterization of complex biological processes. The combined assessment of different tumor features, such

as glucose metabolism, cellularity, and vascularization, opens up possibilities for a more detailed characterization of the primary tumor and for the prognostication of therapy response and clinical outcome. Therefore, PET/MR represents the optimal non-invasive diagnostic tool for a personalized therapeutic approach in head and neck cancer patients.

**Acknowledgment** The authors of this chapter are indebted to Abdulrahman Abdullah Albatly, M.D.

## References

1. Sekine T, de Galiza Barbosa F, Kuhn FP, Burger IA, Stolzmann P, Huber GF, et al. PET+MR versus PET/CT in the initial staging of head and neck cancer, using a trimodality PET/CT+MR system. Clin Imaging. 2017;42:232–9.
2. Huellner MW, Appenzeller P, Kuhn FP, Husmann L, Pietsch CM, Burger IA, et al. Whole-body nonenhanced PET/MR versus PET/CT in the staging and restaging of cancers: preliminary observations. Radiology. 2014;273(3):859–69.
3. Schaarschmidt BM, Heusch P, Buchbender C, Ruhlmann M, Bergmann C, Ruhlmann V, et al. Locoregional tumour evaluation of squamous cell carcinoma in the head and neck area: a comparison between MRI, PET/CT and integrated PET/MRI. Eur J Nucl Med Mol Imaging. 2016;43(1):92–102.
4. Partovi S, Kohan A, Vercher-Conejero JL, Rubbert C, Margevicius S, Schluchter MD, et al. Qualitative and quantitative performance of (1)(8)F-FDG-PET/MRI versus (1)(8)F-FDG-PET/CT in patients with head and neck cancer. AJNR Am J Neuroradiol. 2014;35(10):1970–5.
5. Kuhn FP, Hullner M, Mader CE, Kastrinidis N, Huber GF, von Schulthess GK, et al. Contrast-enhanced PET/MR imaging versus contrast-enhanced PET/CT in head and neck cancer: how much MR information is needed? Journal of nuclear medicine : official publication. Soc Nucl Med. 2014;55(4):551–8.
6. Kubiessa K, Purz S, Gawlitza M, Kuhn A, Fuchs J, Steinhoff KG, et al. Initial clinical results of simultaneous 18F-FDG PET/MRI in comparison to 18F-FDG PET/CT in patients with head and neck cancer. Eur J Nucl Med Mol Imaging. 2014;41(4):639–48.
7. Platzek I, Beuthien-Baumann B, Schneider M, Gudziol V, Langner J, Schramm G, et al. PET/MRI in head and neck cancer: initial experience. Eur J Nucl Med Mol Imaging. 2013;40(1):6–11.
8. Varoquaux A, Rager O, Poncet A, Delattre BM, Ratib O, Becker CD, et al. Detection and quantification of focal uptake in head and neck tumours: (18)F-FDG PET/MR versus PET/CT. Eur J Nucl Med Mol Imaging. 2014;41(3):462–75.
9. Adams S, Baum RP, Stuckensen T, Bitter K, Hor G. Prospective comparison of 18F-FDG PET with conventional imaging modalities (CT, MRI, US) in lymph node staging of head and neck cancer. Eur J Nucl Med. 1998;25(9):1255–60.
10. Stolzmann P, Veit-Haibach P, Chuck N, Rossi C, Frauenfelder T, Alkadhi H, et al. Detection rate, location, and size of pulmonary nodules in trimodality PET/CT-MR: comparison of low-dose CT and Dixon-based MR imaging. Investig Radiol. 2013;48(5):241–6.
11. Togao O, Tsuji R, Ohno Y, Dimitrov I, Takahashi M. Ultrashort echo time (UTE) MRI of the lung: assessment of tissue density in the lung parenchyma. Magn Reson Med. 2010;64(5):1491–8.
12. Tibiletti M, Paul J, Bianchi A, Wundrak S, Rottbauer W, Stiller D, et al. Multistage three-dimensional UTE lung imaging by image-based self-gating. Magn Reson Med. 2016;75(3):1324–32.
13. Ohno Y, Koyama H, Yoshikawa T, Seki S, Takenaka D, Yui M, et al. Pulmonary high-resolution ultrashort TE MR imaging: comparison with thin-section standard- and low-dose computed tomography for the assessment of pulmonary parenchyma diseases. J Magn Reson Imaging. 2016;43(2):512–32.

14. Ter Voert EE, Veit-Haibach P, Ahn S, Wiesinger F, Khalighi MM, Levin CS, et al. Clinical evaluation of TOF versus non-TOF on PET artifacts in simultaneous PET/MR: a dual centre experience. Eur J Nucl Med Mol Imaging. 2017;44(7):1223–33.
15. de Galiza Barbosa F, Delso G, Zeimpekis KG, Ter Voert E, Hullner M, Stolzmann P, et al. Evaluation and clinical quantification of neoplastic lesions and physiological structures in TOF-PET/MRI and non-TOF/MRI - a pilot study. Q J Nucl Med Mol Imaging. 2015. https://www.ncbi.nlm.nih.gov/pubmed/25964058. Epub ahead of print.
16. Wollenweber SD, Delso G, Deller T, Goldhaber D, Hullner M, Veit-Haibach P. Characterization of the impact to PET quantification and image quality of an anterior array surface coil for PET/MR imaging. MAGMA. 2014;27(2):149–59.
17. Svirydenka H, Delso G, Barbosa FG, Huellner MW, Davison H, Fanti S, et al. The effect of susceptibility artifacts related to metal implants on adjacent lesion assessment in simultaneous TOF PET/MR. J Nucl Med. 2017;58(7):1167–73.
18. Zeimpekis KG, Barbosa F, Hullner M, ter Voert E, Davison H, Veit-Haibach P, et al. Clinical evaluation of PET image quality as a function of acquisition time in a new TOF-PET/MRI compared to TOF-PET/CT--initial results. Mol Imaging Biol. 2015;17(5):735–44.
19. Davison H, ter Voert EE, de Galiza Barbosa F, Veit-Haibach P, Delso G. Incorporation of time-of-flight information reduces metal artifacts in simultaneous positron emission tomography/magnetic resonance imaging: a simulation study. Investig Radiol. 2015;50(7):423–9.
20. Sekine T, Ter Voert EE, Warnock G, Buck A, Huellner M, Veit-Haibach P, et al. Clinical evaluation of zero-Echo-time attenuation correction for brain 18F-FDG PET/MRI: comparison with atlas attenuation correction. J Nucl Med. 2016;57(12):1927–32.
21. Delso G, Wiesinger F, Sacolick LI, Kaushik SS, Shanbhag DD, Hullner M, et al. Clinical evaluation of zero-echo-time MR imaging for the segmentation of the skull. J Nucl Med. 2015;56(3):417–22.
22. Wiesinger F, Sacolick LI, Menini A, Kaushik SS, Ahn S, Veit-Haibach P, et al. Zero TE MR bone imaging in the head. Magn Reson Med. 2016;75(1):107–14.
23. von Schulthess GK, Veit-Haibach P. Workflow considerations in PET/MR imaging. J Nucl Med. 2014;55(Supplement 2):19S–24S.
24. Queiroz MA, Huellner MW. PET/MR in cancers of the head and neck. Semin Nucl Med. 2015;45(3):248–65.
25. Vargas MI, Becker M, Garibotto V, Heinzer S, Loubeyre P, Gariani J, et al. Approaches for the optimization of MR protocols in clinical hybrid PET/MRI studies. MAGMA. 2013;26(1):57–69.
26. Dedivitis RA, Denardin OV, Castro MA, Pfuetzenreiter EG Jr. Risk factors for distant metastasis in head and neck cancer. Rev Col Bras Cir. 2009;36(6):478–81.
27. Pipe JG. Motion correction with PROPELLER MRI: application to head motion and free-breathing cardiac imaging. Magn Reson Med. 1999;42(5):963–9.
28. Huellner MW, de Galiza Barbosa F, Husmann L, Pietsch CM, Mader CE, Burger IA, et al. TNM staging of non-small cell lung cancer: comparison of PET/MR and PET/CT. J Nucl Med. 2016;57(1):21–6.
29. Burris NS, Johnson KM, Larson PE, Hope MD, Nagle SK, Behr SC, et al. Detection of small pulmonary nodules with ultrashort echo time sequences in oncology patients by using a PET/MR system. Radiology. 2016;278(1):239–46.
30. Furst S, Grimm R, Hong I, Souvatzoglou M, Casey ME, Schwaiger M, et al. Motion correction strategies for integrated PET/MR. J Nucl Med. 2015;56(2):261–9.
31. Surov A, Stumpp P, Meyer HJ, Gawlitza M, Hohn AK, Boehm A, et al. Simultaneous (18) F-FDG-PET/MRI: associations between diffusion, glucose metabolism and histopathological parameters in patients with head and neck squamous cell carcinoma. Oral Oncol. 2016;58:14–20.
32. Rasmussen JH, Norgaard M, Hansen AE, Vogelius IR, Aznar MC, Johannesen HH, et al. Feasibility of multiparametric imaging with PET/MR in head and neck squamous cell carcinoma. J Nucl Med. 2017;58(1):69–74.
33. Choi SH, Paeng JC, Sohn CH, Pagsisihan JR, Kim YJ, Kim KG, et al. Correlation of 18F-FDG uptake with apparent diffusion coefficient ratio measured on standard and high b value diffusion MRI in head and neck cancer. J Nucl Med. 2011;52(7):1056–62.

34. Gawlitza M, Purz S, Kubiessa K, Boehm A, Barthel H, Kluge R, et al. In vivo correlation of glucose metabolism, cell density and microcirculatory parameters in patients with head and neck cancer: initial results using simultaneous PET/MRI. PLoS One. 2015;10(8): e0134749.
35. Varoquaux A, Rager O, Lovblad KO, Masterson K, Dulguerov P, Ratib O, et al. Functional imaging of head and neck squamous cell carcinoma with diffusion-weighted MRI and FDG PET/CT: quantitative analysis of ADC and SUV. Eur J Nucl Med Mol Imaging. 2013;40(6):842–52.
36. Covello M, Cavaliere C, Aiello M, Cianelli MS, Mesolella M, Iorio B, et al. Simultaneous PET/MR head-neck cancer imaging: preliminary clinical experience and multiparametric evaluation. Eur J Radiol. 2015;84(7):1269–76.
37. Huellner MW, Kuhn FP, Curtin HD. Head and neck cancer. In: von Schulthess GK, editor. Molecular anatomic imaging - PET/CT, PET/MR and SPECT/CT. 3rd ed. Philadelphia: Wolters Kluwer; 2016. p. 341–61.
38. Curtin HD. Detection of perineural spread: fat suppression versus no fat suppression. AJNR Am J Neuroradiol. 2004;25(1):1–3.
39. Platzek I. (18)F-Fluorodeoxyglucose PET/MR imaging in head and neck cancer. PET Clin. 2016;11(4):375–86.
40. Rasmussen JH, Fischer BM, Aznar MC, Hansen AE, Vogelius IR, Lofgren J, et al. Reproducibility of (18)F-FDG PET uptake measurements in head and neck squamous cell carcinoma on both PET/CT and PET/MR. Br J Radiol. 2015;88(1048):20140655.
41. Gunzinger JM, Delso G, Boss A, Porto M, Davison H, von Schulthess GK, et al. Metal artifact reduction in patients with dental implants using multispectral three-dimensional data acquisition for hybrid PET/MRI. EJNMMI Phys. 2014;1(1):102.
42. Buchbender C, Hartung-Knemeyer V, Forsting M, Antoch G, Heusner TA. Positron emission tomography (PET) attenuation correction artefacts in PET/CT and PET/MRI. Br J Radiol. 2013;86(1025):20120570.
43. Ladefoged CN, Hansen AE, Keller SH, Fischer BM, Rasmussen JH, Law I, et al. Dental artifacts in the head and neck region: implications for Dixon-based attenuation correction in PET/MR. EJNMMI Phys. 2015;2(1):8.
44. Chang CY, Yang BH, Lin KH, Liu RS, Wang SJ, Shih WJ. Feasibility and incremental benefit of puffed-cheek 18F-FDG PET/CT on oral cancer patients. Clin Nucl Med. 2013;38(10):e374–8.
45. Rusthoven KE, Koshy M, Paulino AC. The role of fluorodeoxyglucose positron emission tomography in cervical lymph node metastases from an unknown primary tumor. Cancer. 2004;101(11):2641–9.
46. Sekine T, Barbosa FG, Sah BR, Mader CE, Delso G, Burger IA, et al. PET/MR outperforms PET/CT in suspected occult tumors. Clin Nucl Med. 2017;42(2):e88–95.
47. Varoquaux A, Rager O, Dulguerov P, Burkhardt K, Ailianou A, Becker M. Diffusion-weighted and PET/MR imaging after radiation therapy for malignant head and neck tumors. Radiographics. 2015;35(5):1502–27.
48. Becker M, Zaidi H. Imaging in head and neck squamous cell carcinoma: the potential role of PET/MRI. Br J Radiol. 2014;87(1036):20130677.
49. Huellner MW, Sekine T. Hybrid imaging: local staging of head and neck cancer. In: Hodler J, Kubik-Huch RA, von Schulthess GK, editors. Diseases of the brain, head and neck, spine 2016-2019: diagnostic imaging, vol. 1. Heidelberg: Springer; 2016. p. 261–79.
50. Popperl G, Lang S, Dagdelen O, Jager L, Tiling R, Hahn K, et al. Correlation of FDG-PET and MRI/CT with histopathology in primary diagnosis, lymph node staging and diagnosis of recurrency of head and neck cancer. RoFo. 2002;174(6):714–20.
51. Cavaliere C, Romeo V, Aiello M, Mesolella M, Iorio B, Barbuto L, et al. Multiparametric evaluation by simultaneous PET-MRI examination in patients with histologically proven laryngeal cancer. Eur J Radiol. 2017;88:47–55.
52. Yousem DM, Gad K, Tufano RP. Resectability issues with head and neck cancer. AJNR Am J Neuroradiol. 2006;27(10):2024–36.

53. Sekine T, Barbosa F, Delso G, Burger IA, Stolzmann P, Ter Voert E, et al. Local resectability assessment of head and neck cancer: positron emission tomography/MRI versus positron emission tomography/CT. Head Neck. 2017;39(8):1550–8.
54. Chang PC, Fischbein NJ, McCalmont TH, Kashani-Sabet M, Zettersten EM, Liu AY, et al. Perineural spread of malignant melanoma of the head and neck: clinical and imaging features. AJNR Am J Neuroradiol. 2004;25(1):5–11.
55. Schaarschmidt BM, Gomez B, Buchbender C, Grueneisen J, Nensa F, Sawicki LM, et al. Is integrated 18F-FDG PET/MRI superior to 18F-FDG PET/CT in the differentiation of incidental tracer uptake in the head and neck area? Diagn Interv Radiol. 2017;23(2):127–32.
56. Wang K, Mullins BT, Falchook AD, Lian J, He K, Shen D, et al. Evaluation of PET/MRI for tumor volume delineation for head and neck cancer. Front Oncol. 2017;7:8.
57. Queiroz MA, Hullner M, Kuhn F, Huber G, Meerwein C, Kollias S, et al. PET/MRI and PET/CT in follow-up of head and neck cancer patients. Eur J Nucl Med Mol Imaging. 2014;41(6):1066–75.
58. Meerwein CM, Queiroz M, Kollias S, Hullner M, Veit-Haibach P, Huber GF. Post-treatment surveillance of head and neck cancer: pitfalls in the interpretation of FDG PET-CT/MRI. Swiss Med Wkly. 2015;145:w14116.
59. Nakamoto Y, Tamai K, Saga T, Higashi T, Hara T, Suga T, et al. Clinical value of image fusion from MR and PET in patients with head and neck cancer. Mol Imaging Biol. 2009;11(1):46–53.
60. Matthews R, Shrestha P, Franceschi D, Relan N, Kaloudis E. Head and neck cancers: post-therapy changes in muscles with FDG PET-CT. Clin Nucl Med. 2010;35(7):494–8.
61. Muller J, Hullner M, Strobel K, Huber GF, Burger IA, Haerle SK. The value of (18) F-FDG-PET/CT imaging in oral cavity cancer patients following surgical reconstruction. Laryngoscope. 2015;125(8):1861–8.
62. Queiroz MA, Hullner M, Kuhn F, Huber G, Meerwein C, Kollias S, et al. Use of diffusion-weighted imaging (DWI) in PET/MRI for head and neck cancer evaluation. Eur J Nucl Med Mol Imaging. 2014;41(12):2212–21.
63. O'Brien CJ, Smith JW, Soong SJ, Urist MM, Maddox WA. Neck dissection with and without radiotherapy: prognostic factors, patterns of recurrence, and survival. Am J Surg. 1986;152(4):456–63.
64. Leemans CR, Tiwari R, Nauta JJ, van der Waal I, Snow GB. Regional lymph node involvement and its significance in the development of distant metastases in head and neck carcinoma. Cancer. 1993;71(2):452–6.
65. Leemans CR, Tiwari R, Nauta JJ, van der Waal I, Snow GB. Recurrence at the primary site in head and neck cancer and the significance of neck lymph node metastases as a prognostic factor. Cancer. 1994;73(1):187–90.
66. Snyderman NL, Johnson JT, Schramm VL Jr, Myers EN, Bedetti CD, Thearle P. Extracapsular spread of carcinoma in cervical lymph nodes. Impact upon survival in patients with carcinoma of the supraglottic larynx. Cancer. 1985;56(7):1597–9.
67. Johnson JT, Myers EN, Bedetti CD, Barnes EL, Schramm VL Jr, Thearle PB. Cervical lymph node metastases. Incidence and implications of extracapsular carcinoma. Arch Otolaryngol. 1985;111(8):534–7.
68. Heusch P, Sproll C, Buchbender C, Rieser E, Terjung J, Antke C, et al. Diagnostic accuracy of ultrasound, (1)(8)F-FDG-PET/CT, and fused (1)(8)F-FDG-PET-MR images with DWI for the detection of cervical lymph node metastases of HNSCC. Clin Oral Investig. 2014;18(3):969–78.
69. Platzek I, Beuthien-Baumann B, Schneider M, Gudziol V, Kitzler HH, Maus J, et al. FDG PET/MR for lymph node staging in head and neck cancer. Eur J Radiol. 2014;83(7):1163–8.
70. Bruschini P, Giorgetti A, Bruschini L, Nacci A, Volterrani D, Cosottini M, et al. Positron emission tomography (PET) in the staging of head neck cancer: comparison between PET and CT. Acta Otorhinolaryngol Ital. 2003;23(6):446–53.

71. Stuckensen T, Kovacs AF, Adams S, Baum RP. Staging of the neck in patients with oral cavity squamous cell carcinomas: a prospective comparison of PET, ultrasound, CT and MRI. J Craniomaxillofac Surg. 2000;28(6):319–24.
72. Yoon DY, Hwang HS, Chang SK, Rho YS, Ahn HY, Kim JH, et al. CT, MR, US,18F-FDG PET/CT, and their combined use for the assessment of cervical lymph node metastases in squamous cell carcinoma of the head and neck. Eur Radiol. 2009;19(3):634–42.
73. Corey AS, Hudgins PA. Radiographic imaging of human papillomavirus related carcinomas of the oropharynx. Head Neck Pathol. 2012;6(Suppl 1):S25–40.
74. Kendi AT, Magliocca K, Corey A, Nickleach DC, Galt J, Higgins K, et al. Do 18F-FDG PET/CT parameters in oropharyngeal and oral cavity squamous cell carcinomas indicate HPV status? Clin Nucl Med. 2015;40(3):e196–200.
75. Kim SG, Friedman K, Patel S, Hagiwara M. Potential role of PET/MRI for imaging metastatic lymph nodes in head and neck cancer. AJR Am J Roentgenol. 2016;207(2):248–56.
76. Raad RA, Friedman KP, Heacock L, Ponzo F, Melsaether A, Chandarana H. Outcome of small lung nodules missed on hybrid PET/MRI in patients with primary malignancy. J Magn Reson Imaging. 2016;43(2):504–11.
77. Chang ST, Nguyen DC, Raptis C, Menias CO, Zhou G, Wang-Gillam A, et al. Natural history of preoperative subcentimeter pulmonary nodules in patients with resectable pancreatic adenocarcinoma: a retrospective cohort study. Ann Surg. 2015;261(5):970–5.
78. Samarin A, Hullner M, Queiroz MA, Stolzmann P, Burger IA, von Schulthess G, et al. 18F-FDG-PET/MR increases diagnostic confidence in detection of bone metastases compared with 18F-FDG-PET/CT. Nucl Med Commun. 2015;36(12):1165–73.
79. Samarin A, Burger C, Wollenweber SD, Crook DW, Burger IA, Schmid DT, et al. PET/MR imaging of bone lesions--implications for PET quantification from imperfect attenuation correction. Eur J Nucl Med Mol Imaging. 2012;39(7):1154–60.
80. Walter C, Ziebart T, Sagheb K, Rahimi-Nedjat RK, Manz A, Hess G. Malignant lymphomas in the head and neck region--a retrospective, single-center study over 41 years. Int J Med Sci. 2015;12(2):141–5.
81. Heacock L, Weissbrot J, Raad R, Campbell N, Friedman KP, Ponzo F, et al. PET/MRI for the evaluation of patients with lymphoma: initial observations. AJR Am J Roentgenol. 2015;204(4):842–8.
82. Herrmann K, Queiroz M, Huellner MW, de Galiza Barbosa F, Buck A, Schaefer N, et al. Diagnostic performance of FDG-PET/MRI and WB-DW-MRI in the evaluation of lymphoma: a prospective comparison to standard FDG-PET/CT. BMC Cancer. 2015;15:1002.
83. Nagarajah J, Jentzen W, Hartung V, Rosenbaum-Krumme S, Mikat C, Heusner TA, et al. Diagnosis and dosimetry in differentiated thyroid carcinoma using 124I PET: comparison of PET/MRI vs PET/CT of the neck. Eur J Nucl Med Mol Imaging. 2011;38(10):1862–8.
84. Binse I, Rosenbaum-Krumme SJ, Bockisch A. Imaging of differentiated thyroid carcinoma: 124I-PET/MRI may not be superior to 124I-PET/CT. Eur J Nucl Med Mol Imaging. 2016;43(6):1185–6.
85. Vrachimis A, Weckesser M, Schafers M, Stegger L. Imaging of differentiated thyroid carcinoma: (124)I-PET/MRI may not be superior to (124)I-PET/CT. Eur J Nucl Med Mol Imaging. 2016;43(6):1183–4.
86. Vrachimis A, Burg MC, Wenning C, Allkemper T, Weckesser M, Schafers M, et al. [(18)F]FDG PET/CT outperforms [(18)F]FDG PET/MRI in differentiated thyroid cancer. Eur J Nucl Med Mol Imaging. 2016;43(2):212–20.
87. Dercle L, Deandreis D, Terroir M, Leboulleux S, Lumbroso J, Schlumberger M. Evaluation of (124)I PET/CT and (124)I PET/MRI in the management of patients with differentiated thyroid cancer. Eur J Nucl Med Mol Imaging. 2016;43(6):1006–10.
88. Huellner MW, Aberle S, Sah BR, Veit-Haibach P, Bonani M, Schmid C, et al. Visualization of parathyroid hyperplasia using 18F-fluorocholine PET/MR in a patient with secondary hyperparathyroidism. Clin Nucl Med. 2016;41(3):e159–61.

89. Kluijfhout WP, Pasternak JD, Gosnell JE, Shen WT, Duh QY, Vriens MR, et al. 18F Fluorocholine PET/MR imaging in patients with primary hyperparathyroidism and inconclusive conventional imaging: a prospective pilot study. Radiology. 2017;284(2):460–7.
90. van Essen M, Krenning EP, Kooij PP, Bakker WH, Feelders RA, de Herder WW, et al. Effects of therapy with [177Lu-DOTA0, Tyr3]octreotate in patients with paraganglioma, meningioma, small cell lung carcinoma, and melanoma. Journal of nuclear medicine : official publication. Soc Nucl Med. 2006;47(10):1599–606.
91. Lutje S, Sauerwein W, Lauenstein T, Bockisch A, Poeppel TD. In vivo visualization of prostate-specific membrane antigen in adenoid cystic carcinoma of the salivary gland. Clin Nucl Med. 2016;41(6):476–7.
92. Driessen JP, van Kempen PM, van der Heijden GJ, Philippens ME, Pameijer FA, Stegeman I, et al. Diffusion-weighted imaging in head and neck squamous cell carcinomas: a systematic review. Head Neck. 2015;37(3):440–8.
93. King AD, Thoeny HC. Functional MRI for the prediction of treatment response in head and neck squamous cell carcinoma: potential and limitations. Cancer Imaging. 2016;16(1):23.
94. Lambrecht M, Van Calster B, Vandecaveye V, De Keyzer F, Roebben I, Hermans R, et al. Integrating pretreatment diffusion weighted MRI into a multivariable prognostic model for head and neck squamous cell carcinoma. Radiother Oncol. 2014;110(3):429–34.
95. Ng SH, Lin CY, Chan SC, Lin YC, Yen TC, Liao CT, et al. Clinical utility of multimodality imaging with dynamic contrast-enhanced MRI, diffusion-weighted MRI, and 18F-FDG PET/CT for the prediction of neck control in oropharyngeal or hypopharyngeal squamous cell carcinoma treated with chemoradiation. PLoS One. 2014;9(12):e115933.
96. Yun TJ, Kim JH, Kim KH, Sohn CH, Park SW. Head and neck squamous cell carcinoma: differentiation of histologic grade with standard- and high-b-value diffusion-weighted MRI. Head Neck. 2013;35(5):626–31.
97. Houweling AC, Wolf AL, Vogel WV, Hamming-Vrieze O, van Vliet-Vroegindeweij C, van de Kamer JB, et al. FDG-PET and diffusion-weighted MRI in head-and-neck cancer patients: implications for dose painting. Radiother Oncol. 2013;106(2):250–4.
98. King AD, Chow KK, Yu KH, Mo FK, Yeung DK, Yuan J, et al. Head and neck squamous cell carcinoma: diagnostic performance of diffusion-weighted MR imaging for the prediction of treatment response. Radiology. 2013;266(2):531–8.
99. Matoba M, Tuji H, Shimode Y, Toyoda I, Kuginuki Y, Miwa K, et al. Fractional change in apparent diffusion coefficient as an imaging biomarker for predicting treatment response in head and neck cancer treated with chemoradiotherapy. AJNR Am J Neuroradiol. 2014;35(2):379–85.
100. Vandecaveye V, Dirix P, De Keyzer F, de Beeck KO, Vander Poorten V, Roebben I, et al. Predictive value of diffusion-weighted magnetic resonance imaging during chemoradiotherapy for head and neck squamous cell carcinoma. Eur Radiol. 2010;20(7):1703–14.
101. Acampora A, Manzo G, Fenza G, Busto G, Serino A, Manto A. High b-value diffusion MRI to differentiate recurrent tumors from Posttreatment changes in head and neck squamous cell carcinoma: a single center prospective study. Biomed Res Int. 2016;2016:2865169.
102. Hwang I, Choi SH, Kim YJ, Kim KG, Lee AL, Yun TJ, et al. Differentiation of recurrent tumor and posttreatment changes in head and neck squamous cell carcinoma: application of high b-value diffusion-weighted imaging. AJNR Am J Neuroradiol. 2013;34(12):2343–8.
103. Chawla S, Kim S, Dougherty L, Wang S, Loevner LA, Quon H, et al. Pretreatment diffusion-weighted and dynamic contrast-enhanced MRI for prediction of local treatment response in squamous cell carcinomas of the head and neck. AJR Am J Roentgenol. 2013;200(1):35–43.
104. Kim S, Loevner LA, Quon H, Kilger A, Sherman E, Weinstein G, et al. Prediction of response to chemoradiation therapy in squamous cell carcinomas of the head and neck using dynamic contrast-enhanced MR imaging. AJNR Am J Neuroradiol. 2010;31(2):262–8.
105. Shukla-Dave A, Lee NY, Jansen JF, Thaler HT, Stambuk HE, Fury MG, et al. Dynamic contrast-enhanced magnetic resonance imaging as a predictor of outcome in head-and-neck squamous cell carcinoma patients with nodal metastases. Int J Radiat Oncol Biol Phys. 2012;82(5):1837–44.

106. Abdel Razek AA, Gaballa G, Ashamalla G, Alashry MS, Nada N. Dynamic susceptibility contrast perfusion-weighted magnetic resonance imaging and diffusion-weighted magnetic resonance imaging in differentiating recurrent head and neck cancer from postradiation changes. J Comput Assist Tomogr. 2015;39(6):849–54.
107. Baer AH, Hoff BA, Srinivasan A, Galban CJ, Mukherji SK. Feasibility analysis of the parametric response map as an early predictor of treatment efficacy in head and neck cancer. AJNR Am J Neuroradiol. 2015;36(4):757–62.
108. King AD, Chow SK, Yu KH, Mo FK, Yeung DK, Yuan J, et al. DCE-MRI for pre-treatment prediction and post-treatment assessment of treatment response in sites of squamous cell carcinoma in the head and neck. PLoS One. 2015;10(12):e0144770.
109. Abdel Razek AA, Poptani H. MR spectroscopy of head and neck cancer. Eur J Radiol. 2013;82(6):982–9.
110. Bezabeh T, Odlum O, Nason R, Kerr P, Sutherland D, Patel R, et al. Prediction of treatment response in head and neck cancer by magnetic resonance spectroscopy. AJNR Am J Neuroradiol. 2005;26(8):2108–13.
111. King AD, Yeung DK, Yu KH, Mo FK, Hu CW, Bhatia KS, et al. Monitoring of treatment response after chemoradiotherapy for head and neck cancer using in vivo 1H MR spectroscopy. Eur Radiol. 2010;20(1):165–72.
112. Hauser T, Essig M, Jensen A, Laun FB, Munter M, Maier-Hein KH, et al. Prediction of treatment response in head and neck carcinomas using IVIM-DWI: evaluation of lymph node metastasis. Eur J Radiol. 2014;83(5):783–7.
113. Lu Y, Jansen JF, Stambuk HE, Gupta G, Lee N, Gonen M, et al. Comparing primary tumors and metastatic nodes in head and neck cancer using intravoxel incoherent motion imaging: a preliminary experience. J Comput Assist Tomogr. 2013;37(3):346–52.
114. Hauser T, Essig M, Jensen A, Gerigk L, Laun FB, Munter M, et al. Characterization and therapy monitoring of head and neck carcinomas using diffusion-imaging-based intravoxel incoherent motion parameters-preliminary results. Neuroradiology. 2013;55(5):527–36.
115. Paudyal R, Oh JH, Riaz N, Venigalla P, Li J, Hatzoglou V, et al. Intravoxel incoherent motion diffusion-weighted MRI during chemoradiation therapy to characterize and monitor treatment response in human papillomavirus head and neck squamous cell carcinoma. J Magn Reson Imaging. 2017;45(4):1013–23.
116. Mack MG, Balzer JO, Straub R, Eichler K, Vogl TJ. Superparamagnetic iron oxide-enhanced MR imaging of head and neck lymph nodes. Radiology. 2002;222(1):239–44.
117. Mortensen LS, Johansen J, Kallehauge J, Primdahl H, Busk M, Lassen P, et al. FAZA PET/CT hypoxia imaging in patients with squamous cell carcinoma of the head and neck treated with radiotherapy: results from the DAHANCA 24 trial. Radiother Oncol. 2012;105(1):14–20.
118. Servagi-Vernat S, Differding S, Hanin FX, Labar D, Bol A, Lee JA, et al. A prospective clinical study of (1)(8)F-FAZA PET-CT hypoxia imaging in head and neck squamous cell carcinoma before and during radiation therapy. Eur J Nucl Med Mol Imaging. 2014;41(8):1544–52.
119. Hendrickson K, Phillips M, Smith W, Peterson L, Krohn K, Rajendran J. Hypoxia imaging with [F-18] FMISO-PET in head and neck cancer: potential for guiding intensity modulated radiation therapy in overcoming hypoxia-induced treatment resistance. Radiother Oncol. 2011;101(3):369–75.